Int. J. Nano Dimens., 11 (1): 50-57, Winter 2020

ORIGINAL ARTICLE

The effect of Carbon nanotube on the most effective peptide in Alzheimer's disease in the presence of Dimethyl Sulfoxide: *In Silico* approach

Farnaz Jahanbin, Mohammad Reza Bozorgmehr*, Ali Morsali, Safar Ali Beyramabadi

Department of Chemistry, Mashhad Branch, Islamic Azad University, Mashhad, Iran

Received 03 June 2019; revised 12 November 2019; accepted 30 November 2019; available online 30 November 2019

Abstract

Due to the non-polar nature of carbon nanotubes, their use in aqueous environments is limited. Therefore, auxiliary solvents such as dimethyl sulfoxide are used to study the interactions between the amyloid-β peptide and carbon nanotubes. In this work, the interaction of Aβ (1-42), the most effective peptide in the development of Alzheimer's disease, with the carbon nanotube was performed using molecular dynamics simulation method. The simulations were carried out in the presence of various concentrations of dimethyl sulfoxide. The stability change of the salt bridge Lys28-Ala42, used in experimental studies, was investigated as a measure of aggregation tendency. Therefore, the radial distribution function of water oxygen atoms and the atoms involved in the salt bridge were used.

The results show that the peak height of the radial distribution function around the oxygen of the residue Ala42 is greater than that of the Nξ atom of the residue Lys28. By determining the side-chain orientation of the aromatic residues Phe4, Tyr10, Phe19, Phe20 with the carbon nanotube, it was found that the residues Phe4 and Tyr10 have a stronger π-π interaction with the carbon nanotube than the residues Phe19 and Phe20. The results in this study are in good agreement with the experimental data and could be helpful to understand the mechanism of amyloid-β aggregation.

Keywords: *Alzheimer; Hydrophobicity; Peptide; Radial Distribution Function; Salt-Bridge.*

How to cite this article

Jahanbin F, Bozorgmehr MR, Morsali A, Beyramabadi SA. The effect of Carbon nanotube on the most effective peptide in Alzheimer's disease in the presence of Dimethyl Sulfoxide: In Silico approach. Int. J. Nano Dimens., 2020; 11 (1): 50-57.

INTRODUCTION

Alzheimer's disease is a progressive and neurodegenerative disease in which amyloid-β protein has the ability of spatial deformation from soluble to oligomer, protofibril or fibril forms and gets accumulated in the brain in the form of insoluble plaques. The presence of these misfolded amyloid-β proteins in the brain has a direct relationship with neural inflammation and toxicity, which results in the degradation of the nerve system and the onset of Alzheimer's disease [1]. Therefore, several therapeutic strategies proposed to prevent misfolding and aggregation of amyloid-β proteins and help to reverse the process [2, 3]. Researchers have shown that the change in hydrophobic forces can affect the aggregation of amyloid-β proteins [4]. Adding hydrophobic particles including nanotubes can change the hydrophobic forces of the system [5, 6]. Nanotubes and other nanomaterials have been widely recognized in biomedical applications due to their unique physicochemical properties.

The interaction between nanomaterials including carbon nanotubes with Aβ protein has been investigated experimentally and theoretically based on nanotechnology in order to diagnose and treat neurological disorders, such as Alzheimer's and Parkinson's diseases [7, 8]. The nanotube and its derivatives indicate the aggregation pattern of Aβ, including Aβ (1-40) and (1-42) isoforms, but its mechanism is still not well understood [9]. However, investigating the formation of fibril to understand the mechanism of aggregation is necessary [10]. Nanomaterials have been shown to stimulate

* Corresponding Author Email: *bozorgmehr@mshdiau.ac.ir*

the natural conformation of proteins, resulting in undesirable biological effects such as inhibition of protein function and protein fibrillation. On the other hand, it has been shown that nanomaterials may play an important role in reducing the severity of the disease by adsorbing the amyloid peptide and controlling the fibrillation transfers and contractions and inhibiting its conformational transitions and fibrillation [11]. Other studies have shown that low levels of hydrophobic portions of these nanomaterials have an inhibitory effect on the transfer of peptide conformation. The effect of hydrophobic nanotubes on the aggregation of Aβ (1-42) peptide was investigated in the presence and absence of nanotubes by Luo et al, and the secondary structure and stability of the peptide in the presence of nanotubes change were determined. Also, the interaction between the carbon nanotube and the residues Phe20 and Tyr10 of the hydrophobic Aβ peptide was investigated and it has been shown that its effect on the chemical nature of the charged residue Glu11 causes disorder [12]. Because of the difference between the nature of carbon nanotubes and aqueous solvents, their use in aqueous environments is limited. Therefore, auxiliary solvents such as dimethyl sulfoxide (DMSO) are used to study the interactions between the amyloid-β peptide and carbon nanotubes. It has been shown that dimethyl sulfoxide plays an unnatural role on the peptide structure [13].

The denaturation properties of dimethyl sulfoxide are attributed to the tendency of hydrogen bonding to the peptide residues via the sulfoxide functional group and the interaction with hydrophobic residues via methyl groups [14]. Other studies have shown that dimethyl sulfoxide has an effect on the secondary structure of the peptide, so that there is change in the structure of the peptide in the presence of pure DMSO but the fibrillation rate, resulting from the change in the secondary structure, increases at the concentration of 10% DMSO [15].

In this research, the structural change of Aβ (1-42) peptide in the presence of carbon nanotubes in various concentrations of dimethyl sulfoxide was investigated using molecular dynamics simulation method.

MOLECULAR DYNAMICS SIMULATION DETAILS

The four simulation boxes with different dimensions were designed and the Aβ (1-42) peptide molecule was placed in the center of each simulation box. The basic structure of amyloid-β peptide was taken from the protein data bank with the code 1Z0Q. A CNT molecule was added into each box, and then, the boxes were filled with water model SPC216. In each box, the number of 100, 200, 300, and 400 atoms of DMSO solvent were added. Then each simulation box was neutralized with sodium ions. Gromacs software version 5.1.2 and OPLS/AA force field were used for calculations. The steepest descent algorithm was used to optimize the designed systems and to eliminate inappropriate contacts between atoms. To fix a constant temperature and pressure during the simulations, the components of the system were coupled with V-rescale and Nose-Hoover thermostat [16], respectively. LINCS algorithm[17] was employed to fix the chemical bonds between the protein atoms and SETTLE algorithm[18] was employed for the solvent molecules. The PME algorithm was used to calculate electrostatic interactions [19]. Energy minimization was done using the steepest descent method to eliminate the primary kinetic energy in each of the simulation boxes and to eliminate inappropriate contacts between atoms. Each simulation box achieved the two-stage equilibrium in NVT and NPT ensemble. At this stage, the time of equilibration was 10ns with 2fs time step. Finally, molecular dynamics was performed by solving the second Newton equation for 100ns with 2fs time step. Each simulation was repeated four times under the different initial conditions to avoid any dependency on the initial conditions and to increase the accuracy. Therefore, the total time reaches ~2 μs for long MD simulation. The simulation systems and components specifications for each system are reported in Table 1, in which

Table 1. The number and the type of molecules in the simulation boxes.

Box no.	Name of system	Number of Peptid	Number of CNT	Number of DMSO	Dimensions of Box
1	C1D100	1	1	100	9.79774×7.12854×8.84467
2	C1D200	1	1	200	10.11780×7.50029×9.2367
3	C1D300	1	1	300	10.18546×7.66653×9.28662
4	C1D400	1	1	400	10.19853×7.67637×9.29855

the name of each system is the number of carbon nanotubes and the number of dimethyl sulfoxide. For example, in the system C1D100, the number of the nanotube is 1 and the number of dimethyl sulfoxide is 100, and similarly, other names assigned for all the systems.

RESULTS AND DISCUSSION

The orientation of aromatic residues is one of the indicators of amyloid-β aggregation [20, 21]. For this purpose, the orientation of the aromatic amino acids Phe4, Tyr10, Phe19, and Phe20 in Aβ (1-42) peptide with the nanotube was determined in the presence of different concentrations of DMSO and the results are shown in Fig. 1.

According to the figure, it can be seen that the residues Phe4 and Tyr10 have a parallel orientation towards the CNT axis in comparison with the other residues; whereas, in the case of the residues Phe19 and Phe20, the peptide orientation is toward inside of the CNT at low DMSO concentrations and toward outside of the CNT at high DMSO concentrations.

To investigate the stability of the peptide structure, the RMSD value of α-carbon in Aβ (1-42) peptide was obtained using the following equation:

$$RMSD\left(t_1,t_2\right)=\left[\frac{1}{M}\sum_{i=1}^{N}m_i r_i\left(t_1\right)-r_i\left(t_2\right)^2\right]^{\frac{1}{2}} \quad (1)$$

Where $r_i(t)$ is the position of atom i at the time t and $M=\sum_{i=1}^{N}m_i$. The Cα-RMSD results for all the systems are shown in Fig. 2.

The figure shows that the lowest fluctuations in the system C1D200 indicate the higher stability of the peptide Aβ (1-42) and the greatest fluctuations in the systems C1D300 and C1D400, represent the most conformational changes in Aβ (1-42) peptide. From the halfway, the highest RMSD values for the system C1D400 were observed, representing the most unstable system, but fluctuations in other systems decreased and the curves became almost smooth, indicating the systems are in equilibrium. It seems that the addition of DMSO makes the system unstable.

To study the peptide size, the radius of gyration (*Rg*) value of Aβ (1-42) peptide was calculated during the simulation using the following equation:

$$R_g=\left(\frac{\sum_i \left\| r_i \right\|^2 m_i}{\sum_i m_i}\right)^{\frac{1}{2}} \quad (2)$$

Where m_i is the atomic mass of i and r_i is the

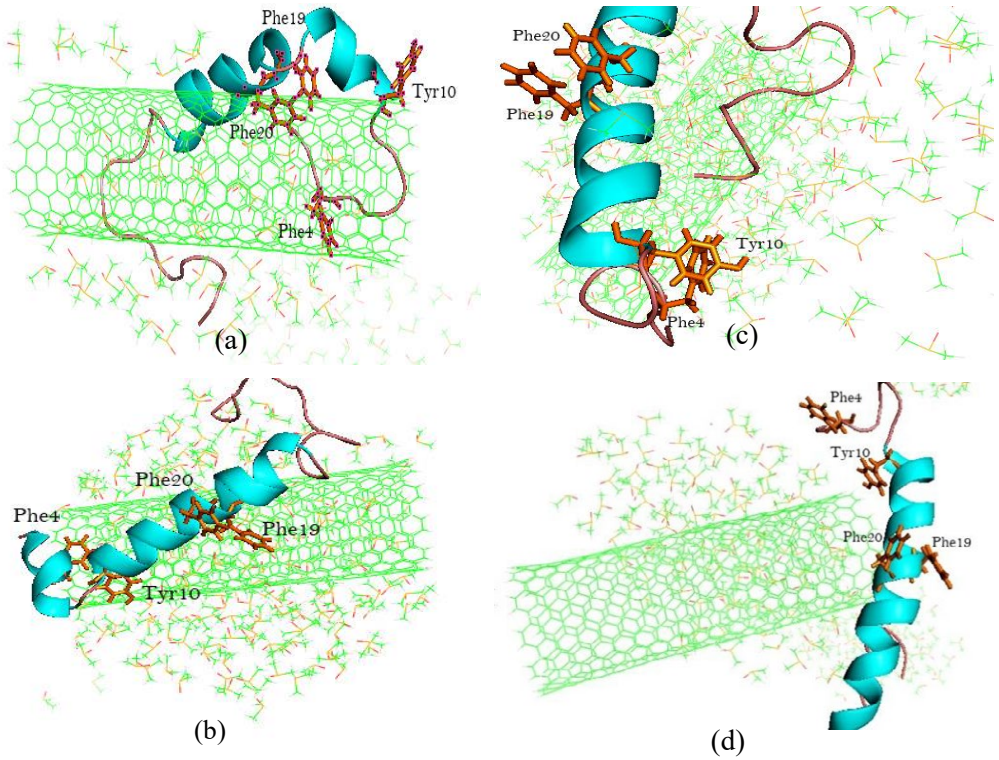

Fig. 1. Snapshot of the protein, nanotube, and DMSO in the systems. (a) C1D100, (b) C1D200, (c) C1D300, (D) C1D400.

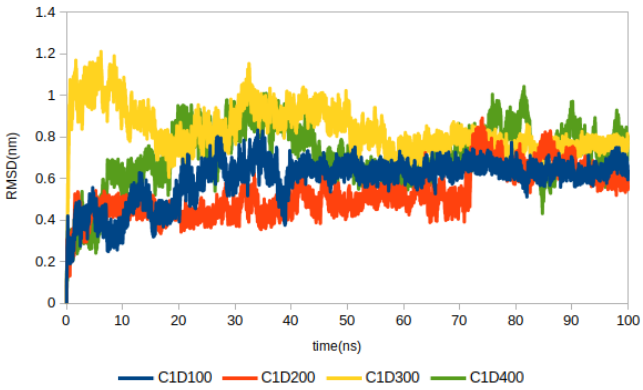

Fig. 2. Cα-RMSD values of Aβ (1-42) in various system.

Fig. 3. *Rg* values (nm) versus time (ps) for the simulated systems.

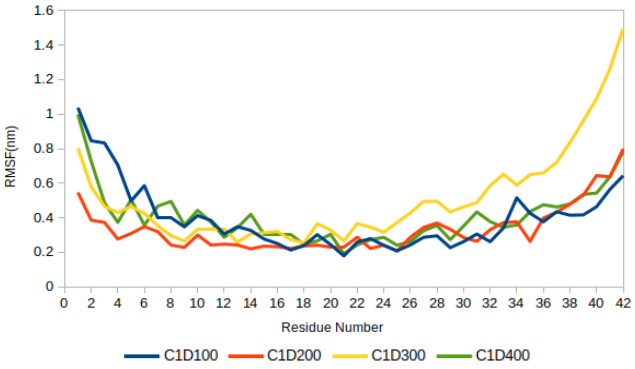

Fig. 4. RMSF values (nm) for Aβ (1-42) residues in simulation systems.

atomic position of *i* relative to the center of the molecule. The results for the designed systems are shown in Fig. 3.

The diagrams show that the lowest fluctuations in the radius of gyration are related to the systems C1D100 and C1D200, and the highest fluctuations are for the systems C1D300 and C1D400, especially the system C1D400. This increase continued to half of the simulation, then, the fluctuations reduced to the end of the simulation, except the system C1D400. These results indicate that increasing the number of DMSO affect the peptide structure and cause the instability of the system. To investigate the flexibility of the Aβ (1-42) residues, the root means square fluctuation (RMSF) values are calculated in all the systems and the results are shown in Fig. 4.

The diagrams show that the flexibility in the curves at the two ends of the peptide is greater than the middle residue. Nevertheless, the minimum flexibility of the residues in the middle region is related to the system C1D200 and the highest flexibility of the residues is related to the systems C1D300 and C1D400, especially the residues Phe19 [21, 22], Glu22, Lys28, Asn27, Gly33 and Val36-Ala42 of the system C1D300. Increasing the number of DMSO in all the systems seems to be effective on the flexibility of the residues Ala42 and Lys28. Since increasing the length of the salt bridge causes the instability of the peptide structure, and as a result of that the possibility of aggregation is reduced, the length of the salt bridge Ala42-Lys28 [23], which has the greatest effect on the stability of the Aβ peptide (1-42), is calculated based on the experimental studies and the results are shown in Fig. 5.

It is observed that the length of the salt bridge LYS28-ALa42 is increasing with increasing the concentration of DMSO, so that the system C1D400 had the largest salt bridge length and the system C1D200 had the smallest salt bridge length compared to the other systems. This result is consistent with the previous analysis. For a closer investigation into the stability of the salt bridge Ala42- Lys28, the distribution of water molecules around O-ALa42 and N_{ξ}-Lys28 atoms forming the salt bridge was also investigated. For this purpose, the radial distribution function, describing the density changes with the distance around a particular atom, was used. The following equation was used to calculate the radial distribution function during the simulation:

$$g(r) = \frac{V}{N^2} \sum_i \sum_{i \neq j} \partial\left(r - r_{ij}\right) \quad (3)$$

Where *V*, *N*, and *r* are the volume, the number of atoms, and the position of them, respectively. r_{ij} is the vector between the center of the atoms *i* and *j*. The peak height in the radial distribution function corresponds to the presence of water molecules surrounding the atoms. The effect of this quantity on the formation of the salt bridge Ala42 - Lys28 around the atoms $N - Lys\,28$ and O-ALA42 was investigated and the results are shown in Figs. 6 and 7, respectively.

As can be seen, the highest peaks of the four concentrations of DMSO are approximately the same, indicating that the interaction tendency between the oxygen atom and the N_{ξ} atom of the

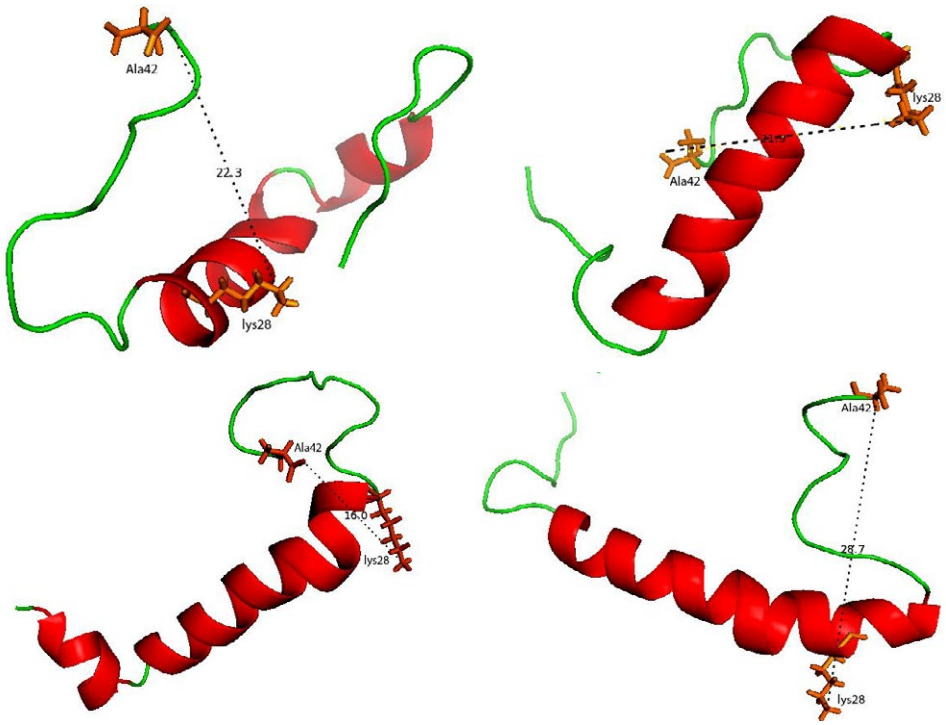

Fig. 5. The length of the salt bridge formed between the atom O of the residue Ala42 and Nξ of the residue LYS28 in all the simulation systems. (a) C1D100, (b) C1D200, (c) C1D300, (D) C1D400.

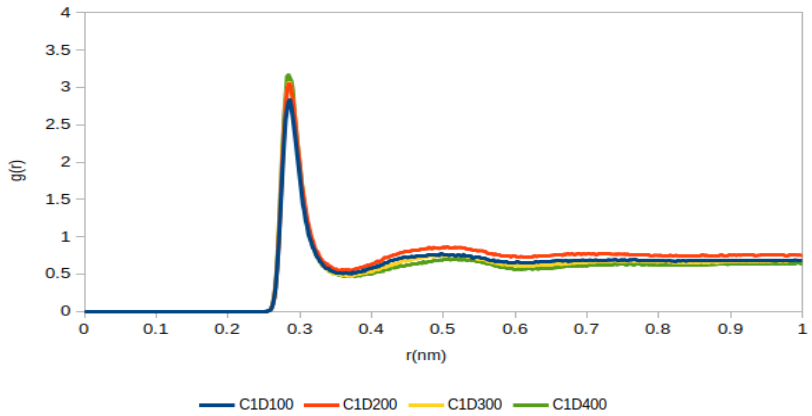

Fig. 6. The plots of the radial distribution function for the water oxygen atoms around.

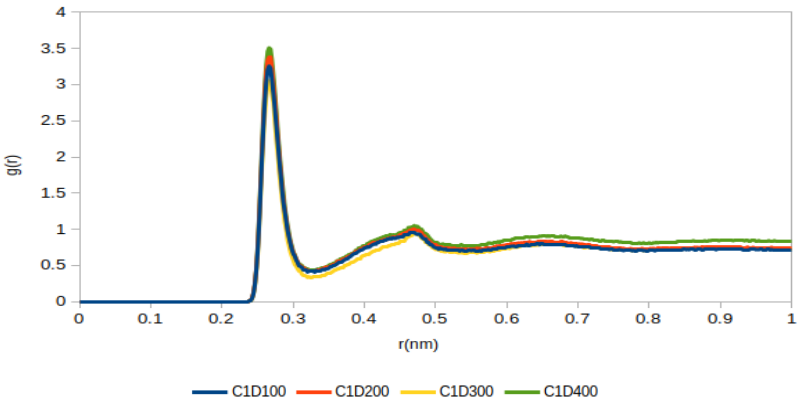

Fig. 7. The plots of the radial distribution function for the water oxygen atoms around.

Table 2. The number of water molecules around the atoms Nξ−Lys28 and O−Ala42 in the first layer of various systems.

system	center	
	$N_\xi - Lys28$	$O \quad - Ala42$
	1st peak	1st peak
C1D100	3.141	2.148
C1D200	3.362	2.212
C1D300	3.253	1.943
C1D400	3.304	2.205

residue Lys28 is almost the same. These results are similar for the oxygen atom of the residue Ala42, except that it has a higher peak height; that means, the more the distance between the oxygen atoms of the water molecules and the N_ξ and O atoms of the residue is, the more solvent mass closer and the peak height will be shorter. However, the number of surrounding water molecules increases which corresponds to the instability of the salt bridge. As a result, the salt bridge in the area of lysine residue is unstable. This is confirmed by the results of Table 2, which determines the number of water molecules in the area of the peaks of the radial distribution function diagram.

Much experimental evidence indicates the major role of some hydrophobic residues in the formation of fibrils [24, 25]. Therefore, the solvent accessible surface area of the residues of Aβ (1-42) peptide was calculated to evaluate the hydrophobicity of the residues in all the designed systems, and the results are shown in Fig. 8.

Accordingly, we find that the solvent accessible surface area of the residues is approximately the same at all concentrations. Since the N-terminal

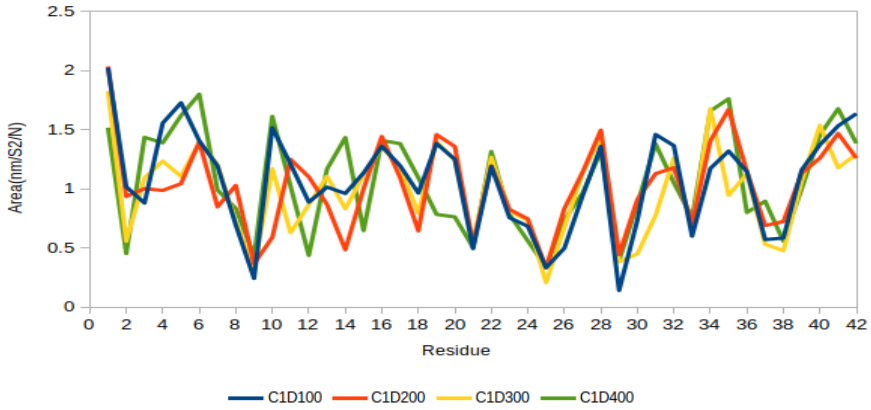

Fig. 8. The plots of the hydrophobic solvent accessible surface area of the residues of Aβ (1-42).

Table 3. The most probable secondary structure for Aβ (1 -42) residues in the simulated systems (C: random coil, H: Helix).

RES NO	C1D100	C1D200	C1D300	C1D400
D	C	C	C	C
A	C	C	C	C
E	C	C	C	C
F	C	H	C	C
R	C	H	C	C
H	C	H	C	C
D	C	H	C	C
S	C	C	C	C
G	C	C	C	C
Y	H	H	C	C
E	H	H	C	H
V	H	H	C	H
H	H	H	C	H
H	H	H	H	H
Q	C	H	H	H
K	H	H	H	H
L	H	H	H	H
V	H	H	H	H
F	H	H	H	H
F	C	H	H	H
A	H	H	H	H
E	H	H	H	H
D	H	H	H	H
V	H	C	H	C
G	H	C	H	H
S	H	C	H	H
N	C	C	H	H
K	C	C	C	H
G	C	C	C	H
A	C	C	C	C
I	C	C	C	C
I	C	C	C	C
G	C	C	C	C
L	C	C	C	C
M	C	C	C	C

of the peptide is inside the membrane, it is hydrophobic in nature. Therefore, when separated from the membrane, it is more sensitive to the aquatic environment. This fact corresponds to the results shown in Fig. 8. The N-terminal of the peptide residues is more sensitive to alcohol change. Finally, the secondary structure of each Aβ (1-42) residue was obtained and the results are reported in Table 3.

According to Table 3, the most helix percentage is in the system C1D200, and the least helix percentage is in the system C1D300. It seems that the tendency to aggregation decreases with the addition of DMSO. Generally, it was observed that most of the residues that are in the random coil structure are in the N-terminal of the peptide and the helix structure is mainly located in the C-terminal of the peptide. These results are consistent with experimental data [26, 27].

CONCLUSION

In this study, the effect of the nanotube on the structure of amyloid-β (1-42), effective in Alzheimer's disease, was investigated in the presence of DMSO. DMSO should be considered as a true bioactive compound whose mechanisms of action might be beneficial against some neurodegenerative conditions. The effects of chronic DMSO on the behavior of neurons and amyloid-β are important to be considered for the development of appropriate therapies for neurodegenerative diseases. Also, this compound is widely used in preclinical and clinical research as it enhances the entrance of water-insoluble drug candidates into the central nervous system. It was found that the flexibility of the peptide residues at the two terminals is more than that of the middle residues. Nevertheless, the minimum flexibility of the residues is related to the system C1D200 and the greatest flexibility of the residues is related to the systems C1D300 and C1D400, especially C1D300 with the greatest flexibility related to the residues Phe19, Glu22, Lys28, Asn27, Gly33, and Val36-Ala42. It was also observed that the

salt bridge length between the residues Lys28 and Ala42 is being increased with increasing the number of DMSO in different systems. The lowest salt bridge length is related to the system C1D200 and the greatest one is for the system C1D400. By determining the side chain orientation of the aromatic residues Phe4, Tyr10, Phe19, Phe20, and Phe20 with the carbon nanotube, it was found that the residues Phe4 and the Tyr10 have greater π-π interaction with the carbon nanotube than that of the residues Phe19 and Phe20. This orientation in the system C1D200 was better than other systems. The results of this study indicate that the amount of auxiliary solvent must be controlled.

DISCLOSURE STATEMENT

All authors declare that they have no conflict of interest in the publication of this manuscript.

REFERENCES

1. Haass C., Selkoe D. J. (2007), Soluble protein oligomers in neurodegeneration: Lessons from the Alzheimer's amyloid β-peptide. *Nat. Rev. Molec. Cell Biol.* 8: 101-106.
2. Gervais F., Paquette J., Morissette C., Krzywkowski P., Yu M., Azzi M., Lacombe D., Kong X., Aman A., Laurin J., Szarek W. A., Tremblay P., (2007), Targeting soluble Aβ peptide with Tramiprosate for the treatment of brain amyloidosis. *Neurobiol. Aging.* 28: 537-547.
3. Salomone S., Caraci F., Leggio G. M., Fedotova J., Drago F., (2012), New pharmacological strategies for treatment of Alzheimer's disease: Focus on disease modifying drugs. *Brit. J. Clinical Pharmacol.* 73: 504-517.
4. Parvaee E., Bozorgmehr M. R., Morsali A., (2019), Role of repulsive forces on self-assembly behavior of amyloid β-peptide (1-40): Molecular dynamics simulation approach. *Physica A: Statistic. Mechan. Applicat.* 513: 524-535.
5. Ghule A. V., Kathir K. M., Kumar T. K. S., Tzing S-H., Chang J-Y., Yu C., Ling Y-C., (2007), Carbon nanotubes prevent *2, 2, 2*-Trifluoroethanol induced aggregation of protein. *Carbon.* 45: 1586-1589.
6. Linse, S., Cabaleiro-Lago C., Xue W-F., Lynch I., Lindman S., Thulin E., Radford Sh-E., Dawson K-A., (2007), Nucleation of protein fibrillation by nanoparticles. *Proceed. Nat. Acad. Sci.* 104: 8691-8696.
7. Baweja L., Balamurugan K., Subramanian V., Dhawan A., (2015), *E*ffect of graphene oxide on the conformational transitions of amyloid beta peptide: A molecular dynamics simulation study. *J. Molec. Graph. Model.* 61: 175-185.
8. Bussy C., Ali-Boucetta H., Kostarelos K., (2012), Safety considerations for graphene: lessons learnt from carbon nanotubes. *Accoun. Chem. Res.* 46: 692-701.
9. Singer S., (1963), The properties of proteins in nonaqueous solvents. *Adv. Protein chem.* 17: 1-68.
10. Karle I. L., Flippen-Anderson J. L., Uma K., Balaram P., (1993), Unfolding of an α-helix in peptide crystals by solvation: Conformational fragility in a heptapeptide. *Biopolymers: Orig. Res. Biomolec.* 33: 827-837.
11. Brambilla D., Verpillot R., Le Droumaguet B., Nicolas J., Taverna M., Kóňa J., Lettiero B., Hashemi SH., De Kimpe L., Canovi M., Gobbi M., Nicolas V., Scheper W., Moghimi S. M., Tvaroška I., Couvreur P., Andrieux K. (2012), PEGylated nanoparticles bind to and alter amyloid-beta peptide conformation: Toward engineering of functional nanomedicines for Alzheimer's disease. *ACS Nano.* 6: 5897-5908.
12. Luo J., Wärmländer S. K., Yu C. H., Muhammad K., Gräslund A., Pieter Abrahams J., (2014), The Aβ peptide forms non-amyloid fibrils in the presence of carbon nanotubes. *Nanoscale.* 6: 6720-6726.
13. Stefansson S., Knight M., Ahn S., (2012), Specific binding of Alzheimer's Aβ peptide fibrils to single-walled carbon nanotubes. *Nanomater. Nanotechnol.* 2: 1-7.
14. Lehmann M., Stansfield R., (1989), Binding of dimethyl sulfoxide to lysozyme in crystals, studied with neutron diffraction. *Biochem.* 28: 7028-7033.
15. Shen C.-L., Murphy R. M., (1995), Solvent effects on self-assembly of amyloid-β peptide. *Biophys. J.* 69: 640-651.
16. Bussi G., Donadio D., Parrinello M., (2007), Canonical sampling through velocity rescaling. *J. Chem. Phys.* 126: 014101.
17. Hess B., Bekker H., Berendsen H. J. C., Fraaije J. G. M., (1998), LINCS: A linear constraint solver for molecular simulations. *J. Comput. Chem.* 18: 1463-1472.
18. Miyamoto S., Kollman P. A., (1992), Settle: An analytical version of the SHAKE and RATTLE algorithm for rigid water models. *J. Comput. Chem.* 13: 952-962.
19. Essmann, U., Perera L., Berkowitz M. L., (1995), A smooth particle mesh Ewald method. *J. Chem. Phys.* 103: 8577-8593.
20. Paravastu A. K., Leapman R. D., Yau W. M., Tycko R., (2008), Molecular structural basis for polymorphism in Alzheimer's β-amyloid fibrils. *Proc. Natl. Acad. Sci. U. S. A.* 105: 18349-18354.
21. Meinhardt J., Sachse C., Hortschansky P., Grigorieff N., Fändrich M., (2009), Aβ (1-40) fibril polymorphism implies diverse interaction patterns in amyloid fibrils. *J. Molec. Biolog.* 386: 869-877.
22. Honarparvar B., Skelton A. A., (2015), Molecular dynamics simulation and conformational analysis of some catalytically active peptides. *J. Molec. Model.* 21: 100-106.
23. Jahanbin F., Bozorgmehr M. R., Morsali A., Beyramabadi S. A., (2019), The effect of different alcohols on the Asp23-Lys28 and Asp23-Ala42 salt bridges of the most effective peptide in Alzheimer's disease: Molecular dynamics viewpoints. *J. Molec. Graph. Model.* 86: 199-206.
24. Liu, R., McAllister C., Lyubchenko Y., Sierks M. R., (2004), Residues 17–20 and 30–35 of beta-amyloid play critical roles in aggregation. *J. Neurosc. Res.* 75: 162-171.
25. Gu L., Ngo S., Guo Z., (2012), Solid-support electron paramagnetic resonance (EPR) studies of Aβ40 monomers reveal a structured state with three ordered segments. *J. Biolog. Chem.* 287: 9081-9089.
26. Zhang S., Zhang S., Iwata K., Lachenmann M. J., Peng J. W., Li S., Stimson E. R., Lu Y., Felix A. M., Maggio J. E., Lee J. P., (2000), The Alzheimer's peptide Aβ adopts a collapsed coil structure in water. *J. Struc. Biol.* 130: 130-141.
27. Lim K. H., Collver H. H., Le Y. T., Nagchowdhuri P., Kenney J. M., (2007), Characterizations of distinct amyloidogenic conformations of the Aβ (1–40) and (1–42) peptides. *Biochem. Biophys. Res. Communic.* 2: 443-449.